

Supporting Information

High Orientation Asymmetric TADF Molecule with 91% Horizontal Dipole Ratio for High-Efficiency Organic Light-Emitting Diodes

Yanyan Liu,^{*a} Xiaoyu Li,^{†a} Jiaji Yang,^{†c} Zixian Wang,^a Shi-Jian Su,^c Zhenguo Chi
^{*b} and Hai-Tao Feng,^{*a}

^a AIE Research Center, Shaanxi Key Laboratory of Phytochemistry, College of Chemistry and Materials Engineering, Baoji University of Arts and Sciences, Baoji 721013, China

^b School of Environmental and Chemical Engineering, Wuyi University, Jiangmen, 529020, China

^c State Key Laboratory of Luminescent Materials and Devices and Institute of Polymer Optoelectronic Materials and Devices, South China University of Technology, Guangzhou 510640, China

I. Experimental Procedures

General Methods

Nuclear magnetic resonance (^1H NMR and ^{13}C NMR) spectra were recorded on Bruker AvanceIII 400HD and 600HD spectrometer. Deuterated chloroform (CDCl_3) or deuterated dichloromethane (CD_2Cl_2) served as the solvent, with tetramethylsilane (TMS) as the internal reference. High resolution mass spectra (HRMS) were acquired from Thermo Orbitrap Tribrid spectrometer. Elemental analyses were performed on a Vario EL elemental analyzer (Elementar). Cyclic voltammetry (CV) measurements were performed using a Bio-Logic VMP300 electrochemical workstation. A 0.1 M solution of tetrabutylammonium hexafluorophosphate (TBAPF₆) in dichloromethane served as the electrolyte, employing a platinum counter electrode and an Ag/AgCl reference electrode (potentials referenced to the ferrocene/ferrocenium couple, Fc/Fc^+). Photoluminescence (PL) spectra and UV-vis absorption spectra were measured using a Shimadzu RF-5301PC spectrometer and a Hitachi U-3900 spectrophotometer, respectively. Transient PL decay curves were recorded using an Edinburgh FLS 980 spectrometer. Absolute photoluminescence quantum yields were determined on Hamamatsu Photonics C9920-02G absolute PL quantum yield measurement system. Differential scanning calorimetry (DSC) was performed using a NETZSCH DSC 214 Polyma DSC2140A-0211-L at a heating rate of $20\text{ }^\circ\text{C min}^{-1}$ under N_2 atmosphere. Thermogravimetric analyses (TGA) were conducted on a TA thermal analyzer (A50) under N_2 atmosphere with a heating rate of $20\text{ }^\circ\text{C min}^{-1}$. Time-dependent density functional theory (TD-DFT) calculations were performed using the Gaussian 09W software package at the B3LYP/6-311G(d,p) level of theory. Natural transition orbital (NTO) and electron density analysis were extracted by the Multiwfn (version 3.8) and visualized using VMD software (version 1.9.3) based on the TD-DFT results.

Materials.

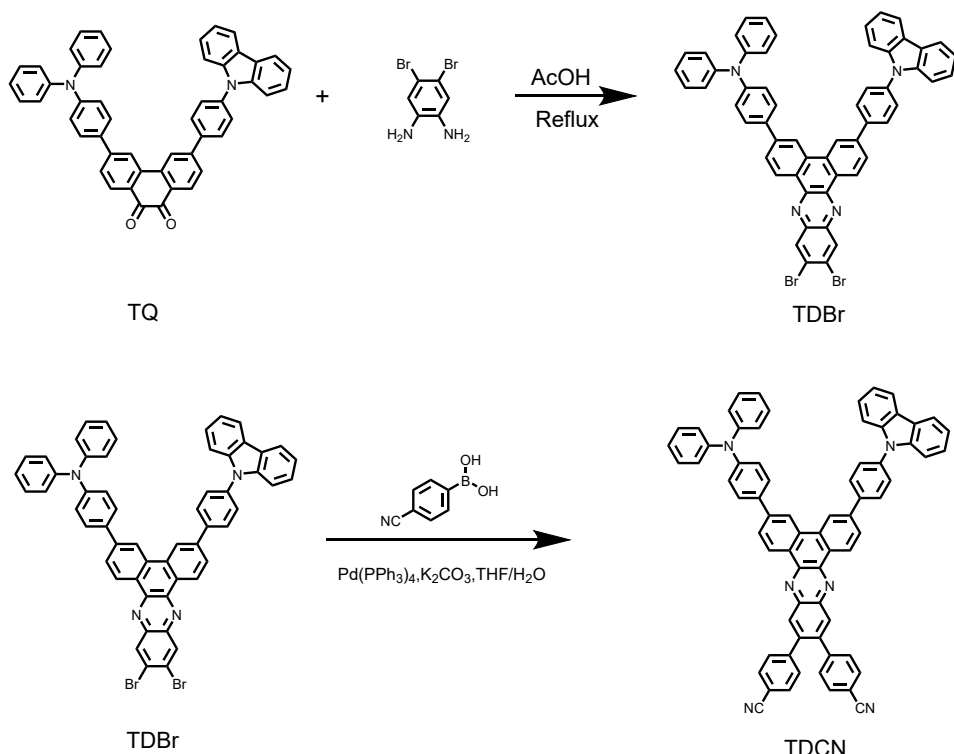
All of the materials were used as received without any purification.

Devices Fabrication and Characterization.

Indium tin oxide (ITO) coated glass substrates were ultrasonically cleaned with detergent, deionized water, acetone and isopropyl alcohol in sequence. After drying, the substrates underwent oxygen plasma treatment for 15 minutes. Then, the ITO substrates were transferred to a thermal evaporation chamber for deposition of organic

and metals layers under high vacuum ($\sim 10^{-5}$ Pa). Organic materials were deposited successively on ITO glass substrate with evaporation rate of 1-2 \AA s^{-1} . The LiF and aluminum (Al) were deposited with evaporation rate of 0.05-0.1 \AA s^{-1} and 1-5 \AA s^{-1} , respectively. The light-emitting area of devices is 3 mm \times 3 mm. Current density-voltage-luminance (J-V-L) characteristics, electroluminescence (EL) spectra and device efficiencies were measured simultaneously using a computer-controlled Keithley 2450 power source and a PR-745 spectral radiometer.

2. Synthesis and characterization



Scheme S1. Synthetic routes of TDCN.

The synthesis method of TQ based on the literature we reported previously^[1].

Synthesis of 4-(6-(4-(9H-carbazol-9-yl)phenyl)-11,12-dibromodibenzo[a,c]phenazin-3-yl)-N,N-diphenylaniline (TDBr):

TQ (3.46 g, 5 mmol) and 4,5-dibromobenzene-1,2-diamine (1.99 g, 7.5 mmol) dissolved in AcOH (50 mL), then the mixture was reflux for 12 h. After cooling to filtered, the crude product was purified by silica gel column chromatography with dichloromethane/n-hexane. TDBr was obtained with 50% yield. ^1H NMR (400 MHz, Chloroform-*d*) δ 9.36 (dd, J = 24.3, 8.3 Hz, 2H), 8.80 (d, J = 25.1 Hz, 2H), 8.65 (s,

2H), 8.19 (dt, J = 7.8, 1.2 Hz, 2H), 8.05 (d, J = 8.4 Hz, 3H), 7.96 (d, J = 8.3 Hz, 1H), 7.83 – 7.67 (m, 4H), 7.55 (dt, J = 8.2, 0.9 Hz, 2H), 7.46 (dt, J = 8.3, 1.2 Hz, 2H), 7.38 – 7.28 (m, 6H), 7.24 (d, J = 1.9 Hz, 2H), 7.22 – 7.14 (m, 4H), 7.12 – 7.02 (m, 2H). ^{13}C NMR (101 MHz, CDCl_3) δ 148.87, 148.14, 143.99, 143.79, 143.40, 142.02, 141.88, 141.44, 140.34, 138.39, 134.64, 133.94, 133.47, 133.17, 130.11, 129.87, 129.70, 129.17, 128.94, 128.24, 128.00, 127.87, 127.69, 127.02, 126.89, 126.76, 125.46, 124.22, 124.20, 124.08, 122.22, 121.49, 121.10, 120.84, 116.39, 110.52. HRMS m/z: [m+1]⁺ calcd for $\text{C}_{56}\text{H}_{34}\text{Br}_2\text{N}_4$, 923.1130, found 923.1200.

Synthesis of 4-(6-(4-(diphenylamino)phenyl)-9,10-dioxo-9,10-dihydrophenanthre-3-yl)benzonitrile (TDCN) :

TDBr (2.77 g, 3 mmol) and 4-cyanophenylboric acid (1.1 g, 7.5 mmol) were dissolved in THF (60 mL), and 2M K_2CO_3 solution (10 mL) was added. Then catalytic amount of $\text{Pd}(\text{PPh}_3)_4$ was added into the mixture under an argon atmosphere. The resulting mixture was stirred at 80 °C for 24 h. After cooling down to ambient temperature, the solvents were evaporated under vacuum and the resulting residue was extracted with DCM and water followed by purification by column chromatography with dichloromethane/n-hexane. TDCN was obtained as a yellow powder in 58% yield. ^1H NMR (400 MHz, Methylene Chloride- d_2) δ 9.31 (dd, J = 15.2, 8.4 Hz, 2H), 8.73 (dd, J = 17.7, 1.8 Hz, 2H), 8.30 (d, J = 4.4 Hz, 2H), 8.13 (dt, J = 7.7, 1.0 Hz, 2H), 7.98 (dq, J = 8.4, 2.1, 1.6 Hz, 3H), 7.90 (dd, J = 8.5, 1.7 Hz, 1H), 7.74 – 7.62 (m, 4H), 7.60 – 7.50 (m, 4H), 7.48 (dt, J = 8.3, 1.0 Hz, 2H), 7.39 (dt, J = 8.3, 1.3 Hz, 2H), 7.37 – 7.19 (m, 10H), 7.20 – 7.13 (m, 2H), 7.13 – 7.07 (m, 4H), 7.06 – 6.95 (m, 2H). ^{13}C NMR (151 MHz, Methylene Chloride- d_2) δ 148.67, 147.92, 144.90, 143.95, 143.79, 143.54, 142.97, 141.90, 141.22, 141.18, 141.11, 139.86, 138.10, 134.22, 133.12, 132.91, 132.58, 131.50, 131.45, 131.07, 129.83, 129.37, 129.08, 128.61, 127.80, 127.57, 127.51, 127.45, 127.29, 126.51, 125.23, 123.94, 123.87, 123.78, 121.98, 121.23, 120.75, 120.58, 118.94, 111.93, 110.23. HRMS m/z: [m+1]⁺ calcd for $\text{C}_{70}\text{H}_{42}\text{N}_6$, 967.3539, found 967.3543. Anal. Calcd for: C, 86.93; H, 4.38; N, 8.69. Found C, 85.76; H, 4.44; N, 8.13.

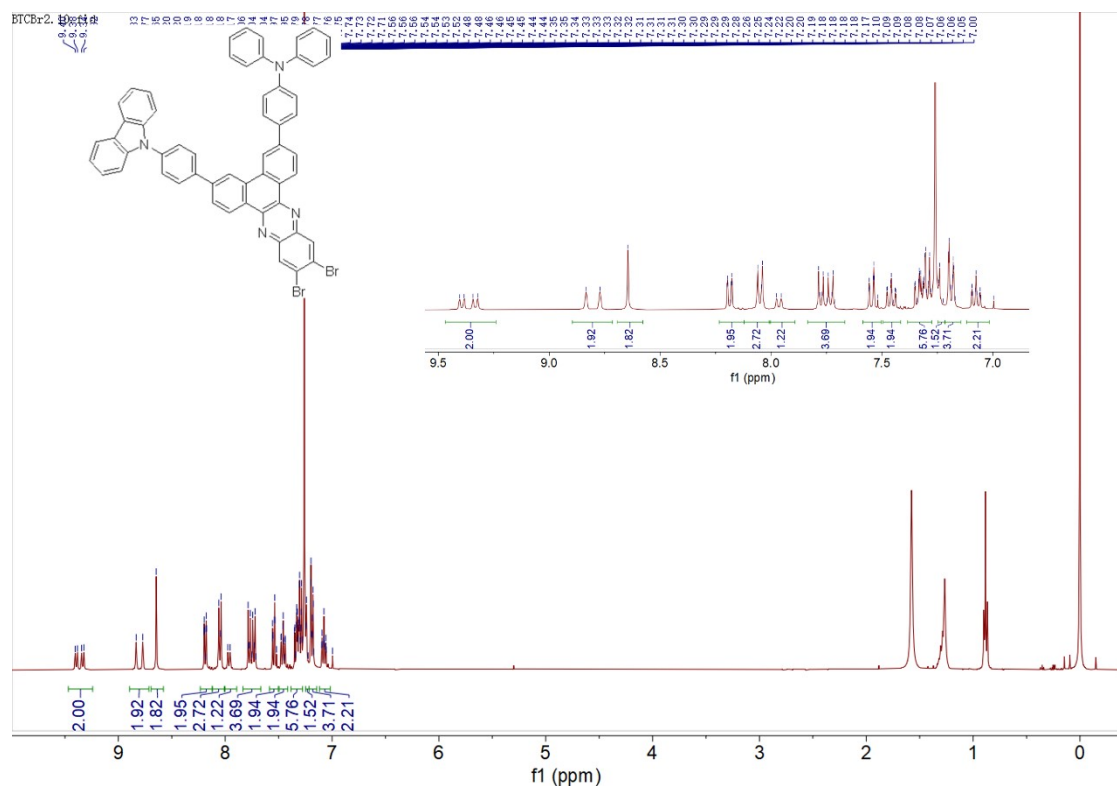


Fig. S1 ^1H NMR spectra of TDBr.

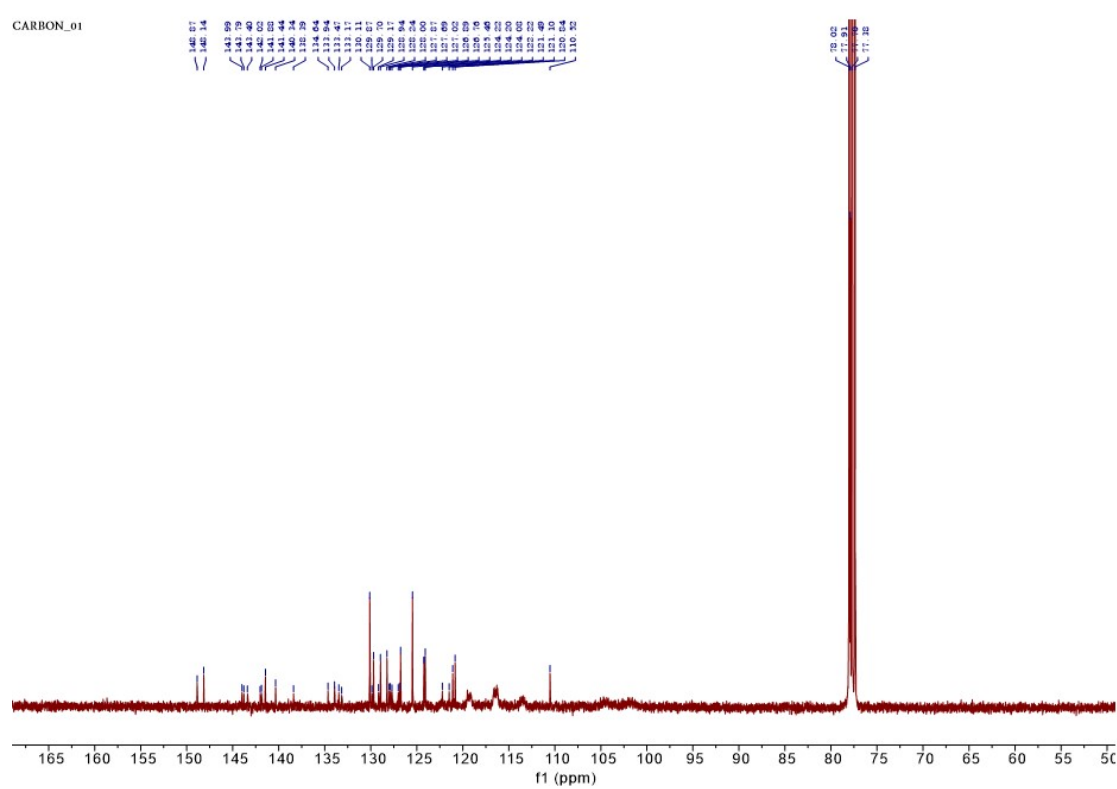


Fig. S2 ^{13}C NMR spectra of TDBr.

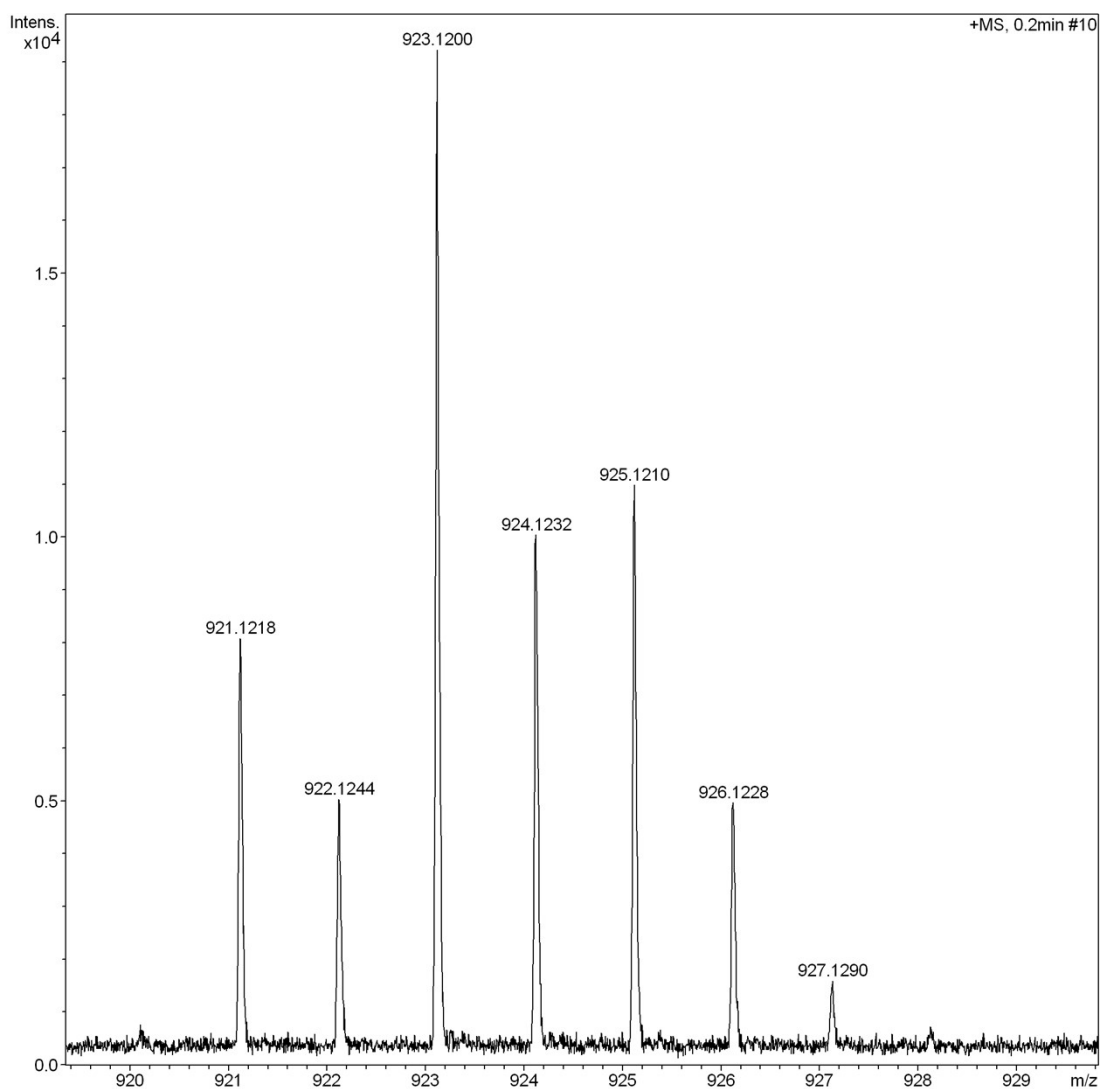


Fig. S3 HRMS spectra of TDBr.

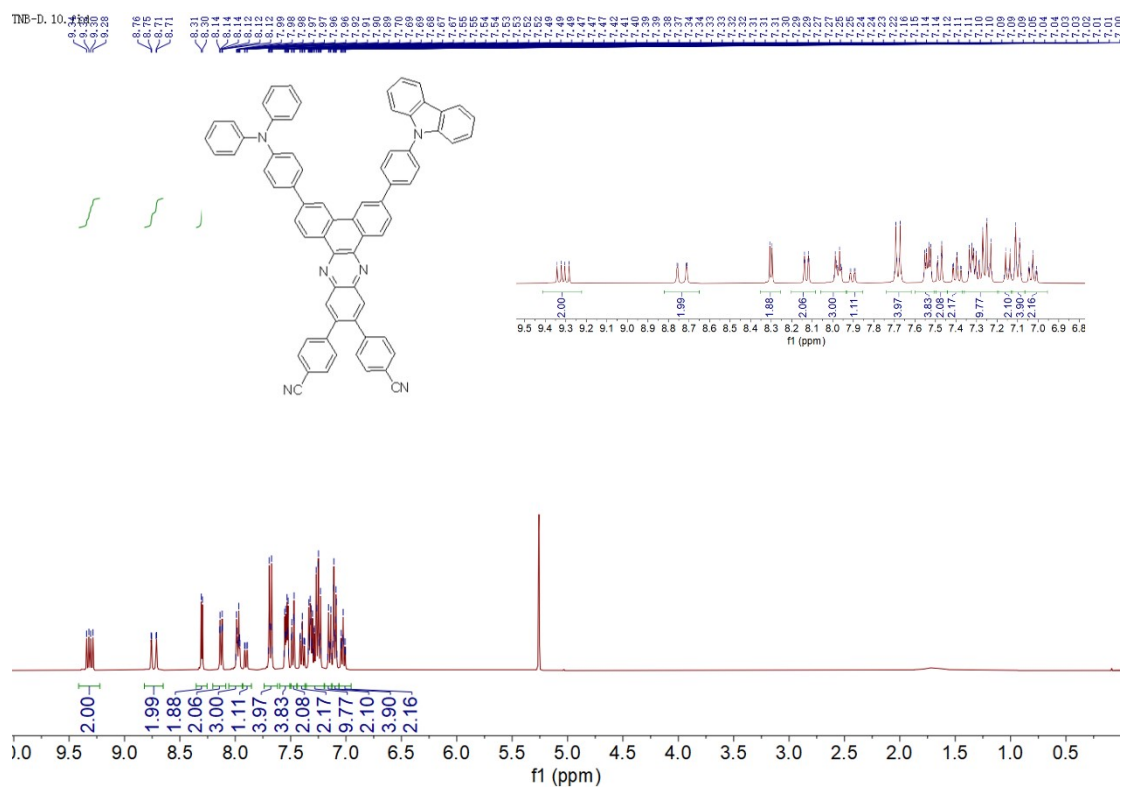


Fig. S4 ^1H NMR spectra of TDCN.

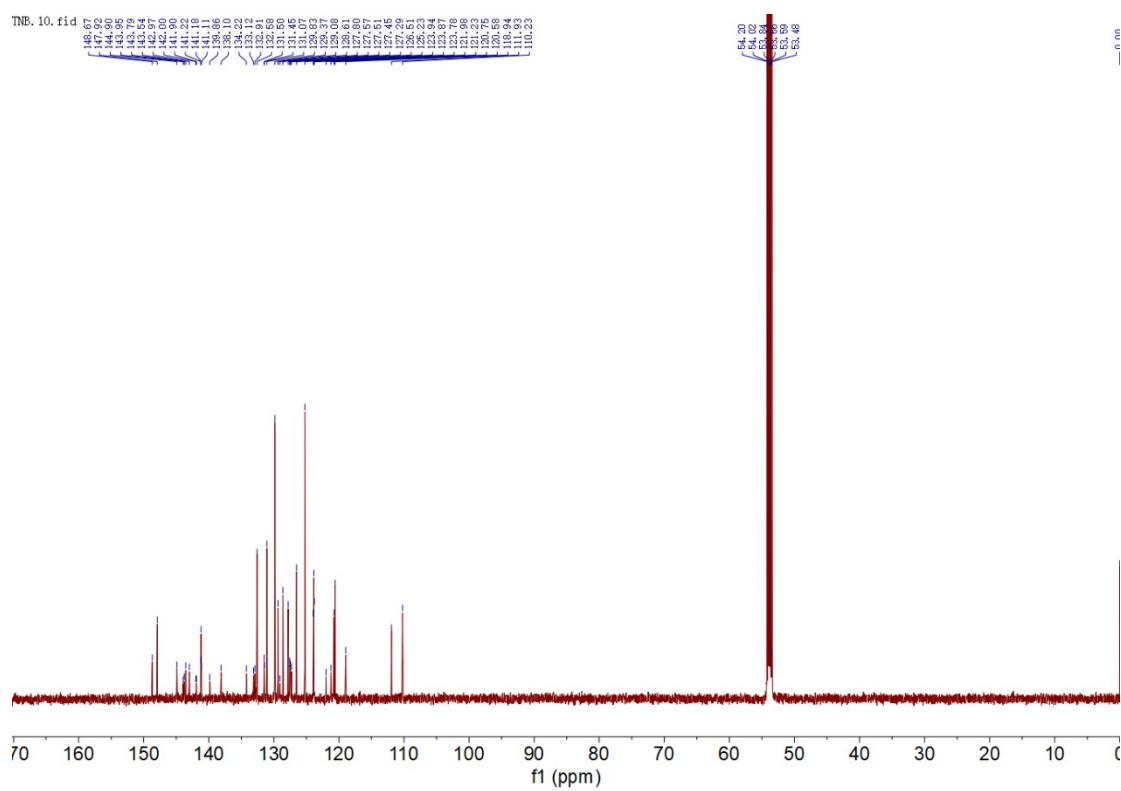


Fig. S5 ^{13}C NMR spectra of TDCN.

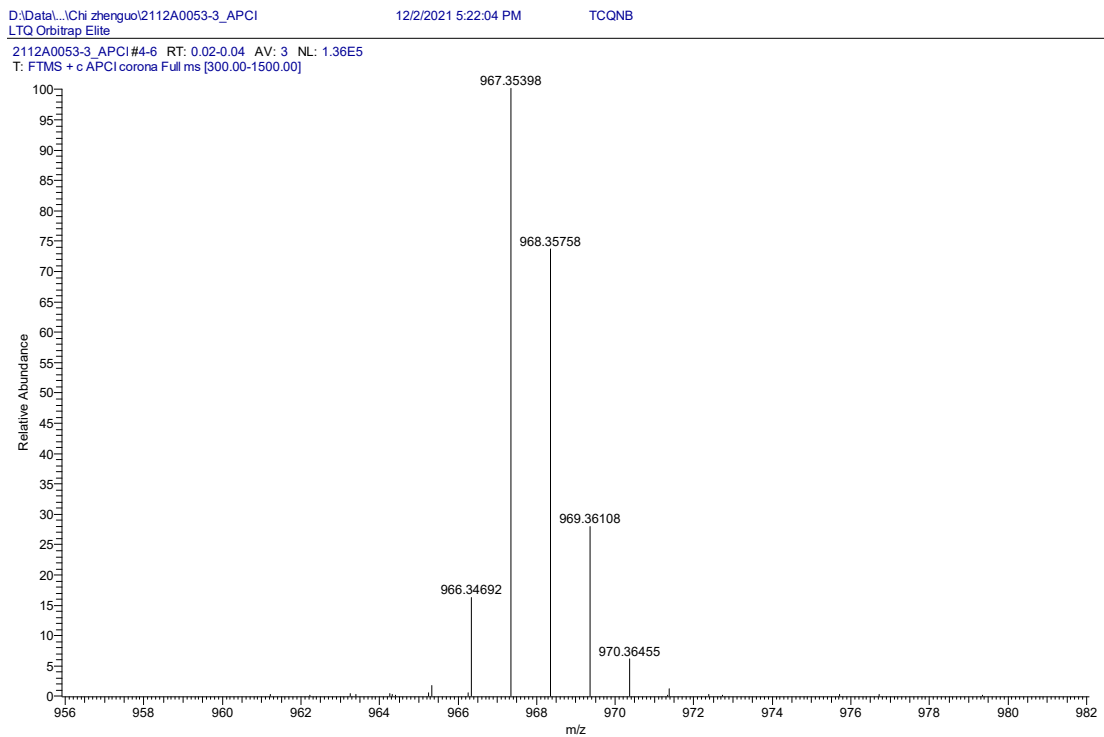


Fig. S6 HRMS spectra of TDCN.

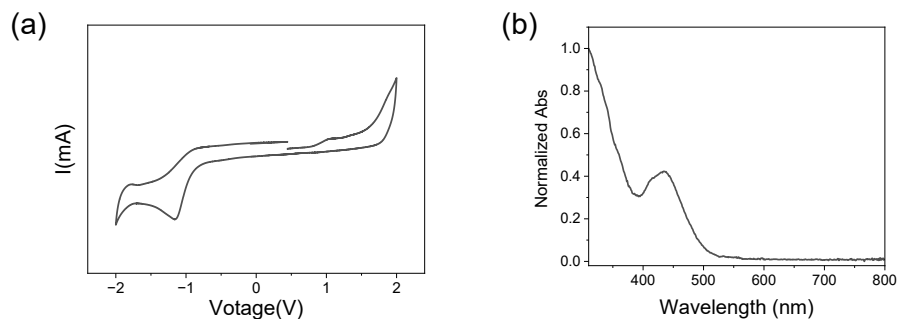


Fig. S7 (a) Cyclic voltammetry measurement of TDCN. HOMO is determined by $\text{HOMO} = -4.8 - (E_{\text{ox}} - E_{1/2(\text{Ferrocene})})$, where E_{ox} is the oxidation potential point, $E_{1/2(\text{Ferrocene})}$ is the oxidation potential of ferrocene (F_c/F_{c+}). (b) UV-vis absorption spectrum in DCM solution (5×10^{-4} mol/L) of TDCN.

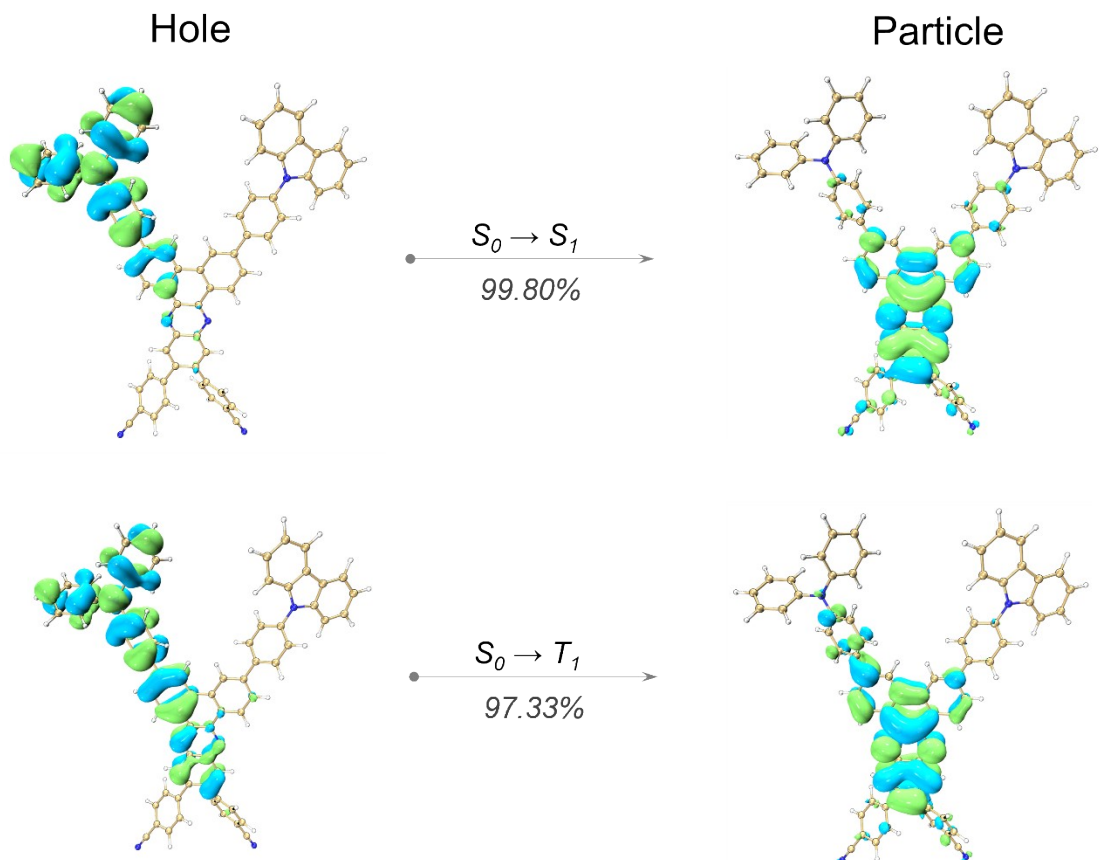


Fig. S8 Natural transition orbitals of TDCN

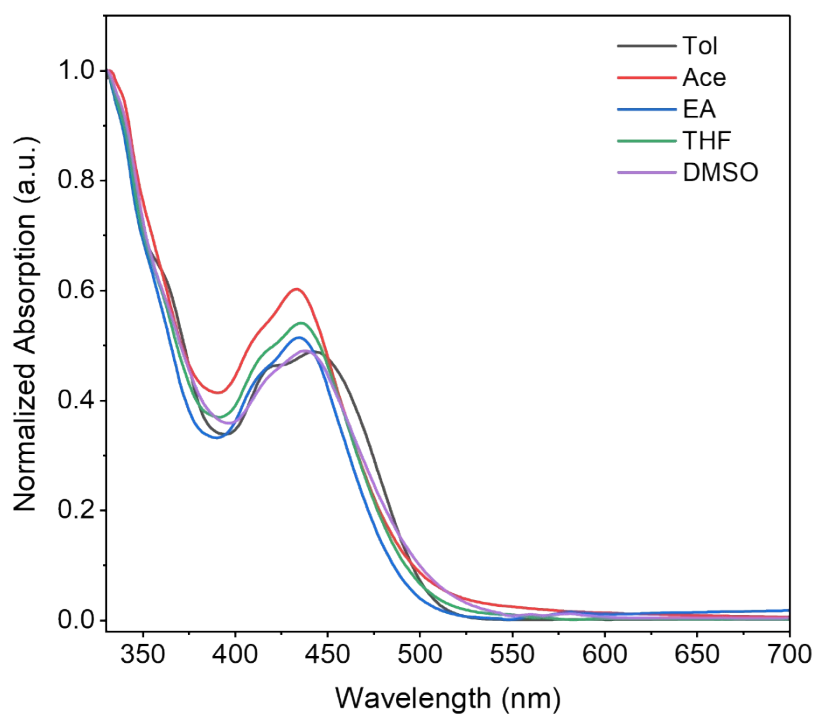


Fig. S9 UV-vis absorption of TDCN in different solvent

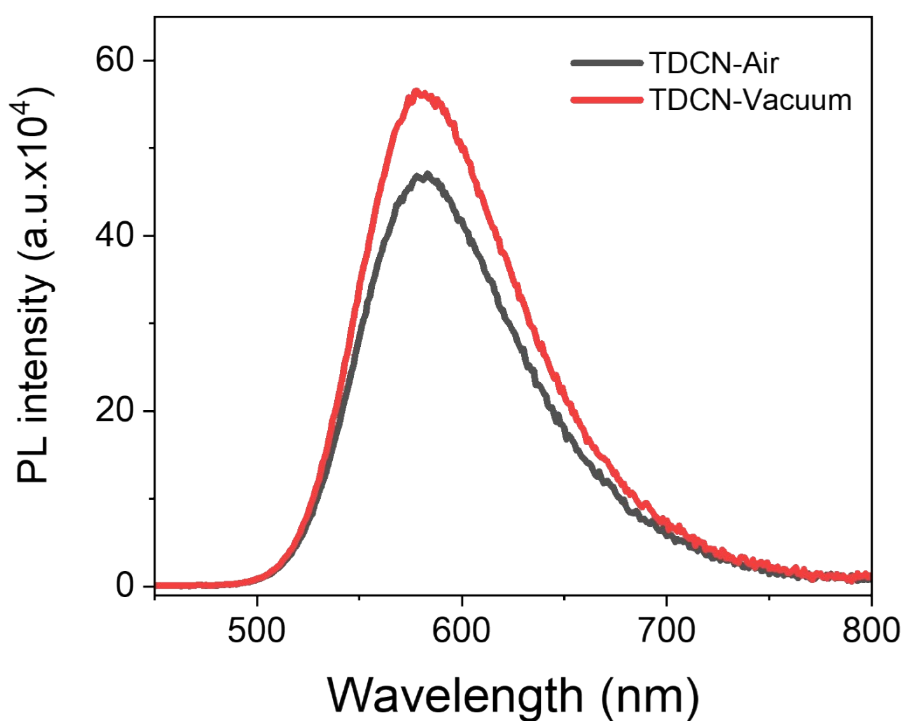


Fig. S10 PL spectra of TDCN in air and vacuum

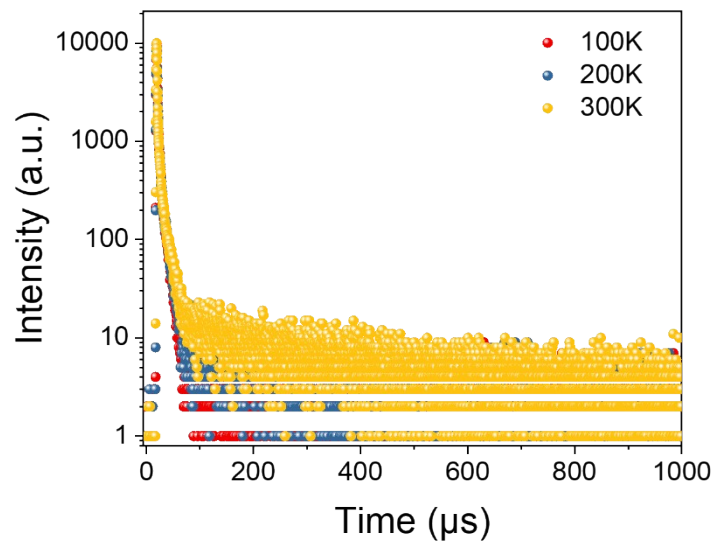


Fig. S11 Temperature-dependent transient PL decays of doped film for TDCN

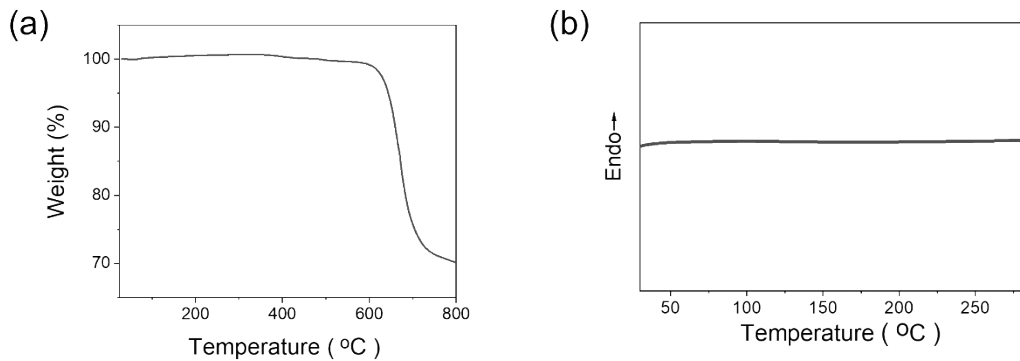


Fig. S12 (a) Thermogravimetric analysis curves and (b) differential scanning calorimetry curve of TDCN

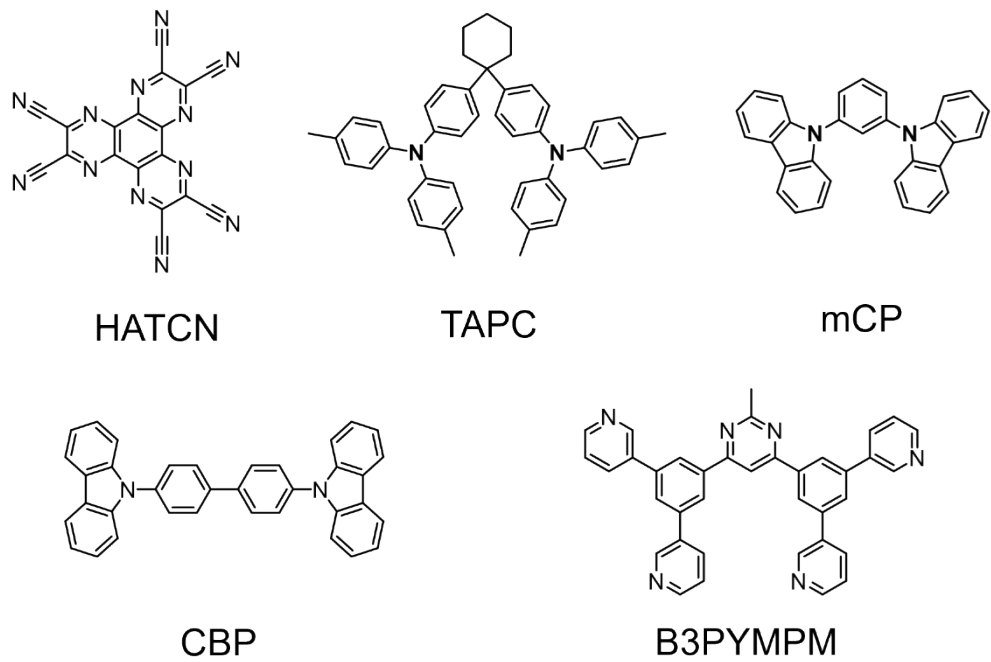


Fig. S13 The chemical structures of corresponding materials used in the OLED devices

Table S2. EL parameters of OLEDs device.

Device	Doping ration	V_{on}	L_{max}	CE_{max}	PE_{max}	EQE_{max}	λ_{EL}	CIE
no.	(%)	(V)	(cd m ⁻²)	(cd A ⁻¹)	(lm W ⁻¹)	(%)	(nm)	(x, y)
Device 1	10	2.6	3569	86.1	76.7	26.4	574	(0.50, 0.50)
Device 2	20	2.6	4382	45.3	54.0	17.7	580	(0.51, 0.48)
Device 3	Non-doped	2.8	3713	5.16	5.2	3.4	610	(0.59, 0.40)

[1] Liu, Y.; Yang, J.; Mao, Z.; Chen, X.; Yang, Z.; Ge, X.; Peng, X.; Zhao, J.; Su, S. J.; Chi, Z. Asymmetric Thermally Activated Delayed Fluorescence Emitter for Highly Efficient Red/Near-Infrared Organic Light-Emitting Diodes. *ACS Appl. Mater. Interfaces* **2022**, (14), 33606–33613.